Differential Scanning Calorimetry and ^2H NMR Studies of the Phase Behavior of Gramicidin–Phosphatidylcholine Mixtures†

Michael R. Morrow*,‡ and James H. Davis§

Department of Physics, Memorial University of Newfoundland, St. John's, Newfoundland, Canada A1B 3X7, and Biophysics Interdepartmental Group and Guelph–Waterloo Program for Graduate Work in Physics, The University of Guelph, Guelph, Ontario, Canada N1G 2W1

Received August 24, 1987; Revised Manuscript Received November 9, 1987

ABSTRACT: The extents of two-phase coexistence in the phase diagrams of mixtures of gramicidin with 1,2-bis(perdeuteriopalmitoyl)-*sn*-glycero-3-phosphocholine (DPPC-d_{62}) and with 1,2-bis(perdeuteriomyristoyl)-*sn*-glycero-3-phosphocholine (DMPC-d_{54}) mixtures have been explored with differential scanning calorimetry (DSC) and deuterium nuclear magnetic resonance (^2H NMR). For both systems, increased gramicidin content causes a decrease in transition enthalpy and a broadening of the peak in excess heat capacity at the transition. In DMPC-d_{54}-based mixtures, the broadening is roughly symmetric about the pure lipid transition temperature. Addition of gramicidin to DPPC-d_{62} extends the excess heat capacity peak on the low-temperature side, resulting in a slightly asymmetric scan. Deuterium NMR spectra showing a superposition of gel and liquid-crystalline components, observed for both mixtures, indicate the presence of two-phase coexistence. For the DPPC-d_{62}-based mixtures, two-phase coexistence is restricted to an approximately 2 °C temperature range below the pure transition temperature. For DMPC-d_{54}-based mixtures, the region of two-phase coexistence is even narrower. For both mixtures, beyond a gramicidin mole fraction of 2%, distinct gel and liquid-crystal contributions to the spectra cannot be distinguished. Along with the broad featureless nature of the DSC scan in this region, this is taken to indicate that the transition has been replaced by a continuous phase change. These results are consistent with the existence of a closed two-phase region having a critical concentration of gramicidin below 2 mol %.

Protein–lipid interaction, and more generally solute–lipid interaction, in the bilayer has been an active field of study on a number of levels. Electron paramagnetic resonance (EPR)[1] (Griffith et al., 1986; Meirovitch et al., 1984), NMR (Bloom & Smith, 1985; Paddy et al., 1981), fluorescence (Rehorek et al., 1985), and vibrational spectroscopy (Mendelsohn et al., 1984; Lee et al., 1984) techniques have all been applied to the study of how intrinsic proteins affect motion and orientational order of surrounding lipid in both the gel and liquid-crystalline phases. Recent reviews have examined the application of spectroscopic techniques to lipid–protein interaction (Devaux & Seigneuret, 1985) and of magnetic resonance to the effect of intrinsic proteins on lipid dynamics (Davis, 1986).

On another level, bilayer component interaction may also be discussed in terms of the modification of bilayer thermodynamics by the presence of intrinsic solute molecules, particularly protein. Examples of this approach include calorimetric studies of the effect of protein molecules on the gel to liquid-crystal transition enthalpy (Semin et al., 1984; Friere et al., 1983) and cooperativity (Heyn et al., 1981). Calorimetry has also been used in the direct measurement of the protein–lipid energy of association (Ramsay et al., 1986). The thermodynamics of lipid–solute interaction may also be addressed by measurements of the lipid–solute phase diagram (Huschilt et al., 1985). A complete picture of lipid–protein interaction must presumably encompass the structural, dynamic, and thermodynamic effects accessible through these various approaches.

Knowledge of the phase diagram should play a role in interpreting thermodynamic results obtained from DSC. Such studies often involve assumptions about the state of spatial organization of bilayer components. In particular, it is important to distinguish situations in which the distribution of bilayer components remains homogeneous throughout the phase change from ones in which phase separation occurs across the range, in temperature, of the transition. It is possible, for example, that the concept of cooperative unit often used to interpret the width of transitions would have to be applied rather differently to cases in which the transition takes place via two-phase coexistence. Accordingly, such studies generally stand to benefit from determination and understanding of the phase diagram for the system of interest in the appropriate region of temperature–solute concentration space. Indeed, thermodynamic details of the component interactions may be directly obtainable from a phase diagram with application of a suitable model for lipid–solute mixing (Lee, 1977; Cheng, 1980).

Recently, ^2H NMR spectral difference spectroscopy has been used to map part of the phase diagram of DPPC-d_{62}–synthetic polypeptide mixtures, thus demonstrating the presence of two-phase coexistence in this system (Huschilt et al., 1985). This approach assumes that within the two-phase coexistence region of a phase diagram, the ^2H NMR spectrum of labeled lipid is a superposition of distinct gel and liquid-

† Supported by grants from the Natural Sciences and Engineering Research Council of Canada.

* Correspondence should be addressed to this author.
‡ Memorial University of Newfoundland.
§ The University of Guelph.

[1] Abbreviations: EPR, electron paramagnetic resonance; ^2H NMR, deuterium nuclear magnetic resonance; DSC, differential scanning calorimetry; DMPC-d_{54}, 1,2-bis(perdeuteriomyristoyl)-*sn*-glycero-3-phosphocholine; DPPC-d_{62}, 1,2-bis(perdeuteriopalmitoyl)-*sn*-glycero-3-phosphocholine; T_{2e}, quadrupole echo decay time; DSPC, 1,2-distearoyl-*sn*-glycero-3-phosphocholine; Tris, tris(hydroxymethyl)aminomethane.

0006-2960/88/0427-2024$01.50/0

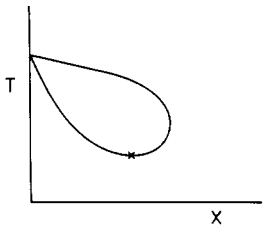

FIGURE 1: Schematic sketch of a partial phase diagram displaying a lower consolute point.

crystal end-point spectra proportioned according to the lever rule. As pointed out (Huschilt et al., 1985), the technique is only applicable if exchange between domains of the coexisting phases is slow enough that the spectral components remain distinct.

Phase diagrams of the lipid–synthetic peptide system, obtained in this way, along with DSC results on these mixtures have been compared to model results based on regular solution theory (Morrow et al., 1985). Some aspects of the observed phase behavior were not reproduced by this modeling. For larger protein concentration in particular, it was found that excess heat capacity observed via DSC could extend beyond the highest temperature for which distinct gel and liquid-crystal spectral components were observed to coexist and, in some cases, beyond the pure lipid transition temperature. This observation was taken to indicate a continuous phase change taking place beyond the boundaries, in the phase diagram, of two-phase coexistence.

Figure 1 shows a type of phase diagram in which two-phase coexistence is replaced, with increasing solute concentration, by a region of continuous phase change. On phase diagrams of this type, the extreme point beyond which two-phase coexistence disappears is the critical mixing point or the consolute point. Such phase diagrams have appeared in discussions of lipid–protein systems. For example, Pink and Chapman (1979) display such a phase diagram for a lattice model calculation on mixtures of DMPC and a large protein. This phase diagram is further discussed in the review by Abney and Owicki (1985). In another recent review, Tenchov (1985) includes such a phase diagram in a sequence of schematic drawings illustrating various possibilities for binary mixtures. Scott and Cheng (1979) modeled gramicidin–DMPC mixtures as two-dimensional systems of hard disks and found that the transition disappeared in a critical point at a polypeptide concentration of 12 mol %. They did not, however, construct a phase diagram using this model. Critical mixing is observed in some fluid mixtures (Streett, 1974) and can be obtained theoretically from models for van der Waals mixtures (van Konynenburg & Scott, 1980).

It is interesting to consider how the presence of a critical concentration might affect the results of DSC experiments on near-critical mixtures. DSC experiments have been simulated by using a Ginsburg–Landau model with parameters chosen to yield a phase diagram with a critical mixing point (J. P. Whitehead and M. R. Morrow, unpublished calculation). At a solute concentration well below the critical concentration, the simulated DSC scan displays a small discontinuity in excess heat capacity as the temperature crosses the lower boundary of the two-phase region. Within the two-phase region, the heat capacity rises and then drops sharply as the temperature passes the upper boundary of the two-phase region. The resulting scan displays the characteristic asymmetric shape found in DSC simulations based on regular mixing thermodynamics (Morrow et al., (1985). In the neighborhood of the critical concentration, the simulated scan shows a similar asymmetric shape, somewhat broadened, superimposed on a broad pedestal extending beyond the boundaries of two-phase coexistence. The broad pedestal was not seen in simulations based on regular solution theory. At concentrations just beyond the limit of the two-phase region, a continuous phase change remains, resulting in a broad featureless peak in the excess heat capacity. The transition enthalpy obtained by integrating the excess heat capacity decreases with increasing solute concentration in the way normally observed for lipid–protein mixtures.

In order to explore conditions under which two-phase coexistence gives way to continuous phase change, it is useful to examine systems in which the solute perturbs the bilayer in different ways and to different extents. Bilayers containing the channel-forming polypeptide gramicidin are often used as a model for protein–lipid interaction studies. Phase diagram studies on such a system represent a logical extension of the previous bilayer-spanning synthetic peptide studies.

Gramicidin is known to form dimers which span the membrane bilayer to form ion channels. While some details of the conformation of gramicidin in the bilayer are still debated (Arseniev et al., 1985), it is generally accepted that the conductive form of the channel is a head to head dimer of $\pi_{L,D}$ helices (Urry et al., 1983; Weinstein et al., 1985; Wallace, 1986). Gramicidin is particularly suitable for phase diagram studies in that, due to its extreme hydrophobicity, it partitions almost entirely into the lipid bilayer. On the other hand, gramicidin within the bilayer is believed to participate in a monomer–dimer equilibrium (Wallace et al., 1981; Elliot et al., 1983; Ring, 1986). Perturbation of the bilayer due to hydrophobic mismatch may be slightly different for the monomer and dimer. The effect of the monomer–dimer equilibrium, in turn, might be sensitive to bilayer thickness and would need to be considered in any detailed modeling of the phase behavior for this system.

Gramicidin has been employed in a number of studies of lipid–protein interaction. Tanaka and Freed (1985) applied spectral simulation techniques (Meirovitch et al., 1984) to EPR studies on DPPC–gramicidin mixtures. In the gel phase, they observed a disordering of the first few layers of lipid surrounding the gramicidin dimer. In the liquid-crystal phase, for concentrations below 4 mol %, they did not see evidence for an immobilized component in macroscopically aligned samples. They also commented on the broadening, by gramicidin, of the two-phase region associated with the gel to liquid-crystal transition. Lee et al. (1984) reported difference infrared spectroscopic studies of gramicidin–DMPC-d_{54} mixtures. These were taken to indicate partial ordering of the lipid chains by gramicidin above the pure lipid transition temperature. Below the transition, gramicidin was observed to partially disorder the lipid chains. Chapman et al. (1977) applied a variety of techniques, including Raman, EPR, and DSC, to gramicidin-containing bilayers of both DMPC and DPPC. Above the pure lipid transition temperature, the Raman studies indicated some ordering of the phospholipid chains even at low polypeptide concentration. The EPR spectra, above about 17 mol %, were interpreted in terms of a lipid population with bulk liquid-crystal properties and a population of more rigid lipid. The DSC experiments showed a linear decrease in transition enthalpy and a broadening of the transition with gramicidin concentration. Rice and Oldfield (1979) examined the ^2H NMR spectra of specifically deuteriated DMPC in bilayers containing gramicidin up to about 43 mol %. All of their reported measurements are at a sample temperature of 30 °C. Up to a gramicidin content

of 6 mol %, quadrupole splitting was observed to increase, indicating partial ordering of the lipid chains by the polypeptide. Beyond this concentration, the splittings were found to decrease. They also reported the observation of very short quadrupole echo decay times, T_{2e}, in some of the mixtures. On the basis of spin–lattice relaxation in the rotating frame, Cornell et al. (1982) concluded that the presence of gramicidin in the bilayer resulted in low-frequency (10^5–10^7 Hz) motions in the bilayer. Although its existence is implied by the calorimetric and EPR experiments discussed, the extent of the two-phase region separating gel and liquid-crystal phases has not been directly investigated for gramicidin–lipid mixtures.

In this paper, we describe DSC and ^{2}H NMR studies on a series of bilayer mixtures containing gramicidin D (Dubos) and either DMPC-d_{54} or DPPC-d_{62}. We have employed both lipids in light of the suggestion by Wallace et al. (1981) that the dimerization constant for gramicidin might differ between DMPC and DPPC such that thinner bilayers, including DMPC, are able to accommodate conducting dimers while thicker bilayers, including DPPC, destabilize the conducting form of the dimer. Where possible, we use spectral subtraction to extract boundaries of two-phase coexistence. Outside of the region of two-phase coexistence, it is not possible to decompose spectra into gel and liquid-crystal end-point contributions. We discuss the observed limits of two-phase coexistence in terms of a phase diagram containing a critical mixing point and comment on how such a phase diagram might be consistent with calorimetric results on this system and the previously studied synthetic polypeptide–DPPC system. We also report a strong dependence of the first spectral moment on quadrupole echo delay time for gramicidin-rich mixtures just below the pure lipid transition temperature.

Materials and Methods

The phospholipids DPPC-d_{62} and DMPC-d_{54} were synthesized as described by Gupta et al. (1977). Gramicidin D (Dubos) was purchased from Calbiochem-Behring (La Jolla, CA) and used without further purification. Stock solutions of each lipid and gramicidin were prepared in ethanol. Samples were generally prepared by combining appropriate volumes of the lipid gramicidin solutions. In addition, three DMPC-d_{54}- and two DPPC-d_{62}-containing samples were prepared by dissolving appropriate dry weights of lipid and gramicidin in ethanol. Mixtures in solution were dried by rotary evaporation followed by pumping at room temperature.

For the purpose of calculating sample concentration, both deuteriated phospholipids were assumed to carry two waters of hydration, giving formula weights of 767 and 832 for DMPC-d_{54} and DPPC-d_{62}, respectively. The formula weight for gramicidin D (Dubos) was taken, from the Calbiochem-Behring catalogue, to be 2000. A series of nine gramicidin–DMPC-d_{54} samples were prepared with gramicidin mole fractions ranging up to x = 0.034. Seven gramicidin–DPPC-d_{62} samples were prepared with gramicidin mole fractions ranging to x = 0.025.

NMR samples were typically 60–70 mg of the gramicidin–lipid mixture hydrated with 100–150 μL of 0.05 M Tris buffer at pH 6.9. Samples were mixed by hand in 8-mm diameter by 25-mm-long NMR tubes using a fine glass stirring rod. For each sample, spectra were obtained for a series of temperatures beginning about 12 °C above the transition and ending about 20 °C below the transition. Each sample thus remains in the liquid-crystal phase for about 10 h before passing through the region of the transition temperature. This procedure allows equilibrium mixing and hydration of each sample prior to the collection of spectra in the neighborhood

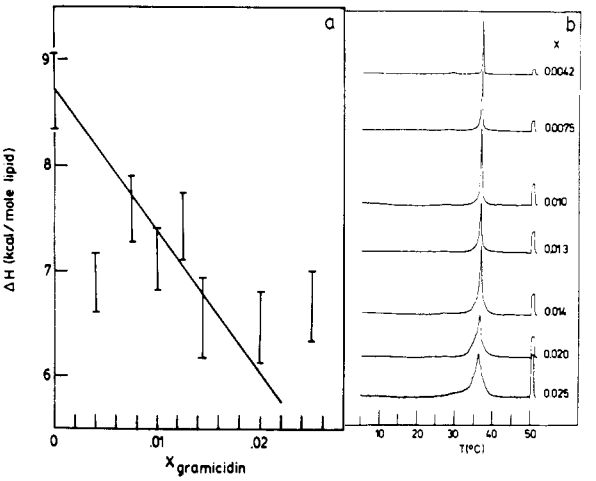

FIGURE 2: DSC results for a series of gramicidin–DPPC-d_{62} multilamellar vesicle samples. (a) Transition enthalpy per mole of lipid versus gramicidin mole fraction. (b) DSC traces for this series. Each scan ends with a calibration pulse.

of the transition. NMR experiments on a given sample were typically completed in less than 48 h. NMR spectra of pure DMPC-d_{54} samples in both Tris and phosphate buffers were compared over the full temperature range used in order to rule out the possibility of any sensitivity to the type of buffer. ^{2}H NMR quadrupole echo experiments were carried out in a superconducting magnet at 41.3 MHz using techniques which have previously been described (Huschilt et al., 1985). Experiments were normally performed with a $\pi/2$ pulse length of 3.25 μs and a quadrupole echo delay of 35 μs. In addition, one series of gramicidin–DMPC-d_{54} experiments was performed with a delay of 50 μs. The ^{2}H NMR spectral difference technique has been described by Huschilt et al. (1985).

Before preparation of the NMR sample, an approximately 5-mg portion of each mixture was separated and placed in solid sample DSC cells. These samples were hydrated, in the cell, with about 20 μL of the Tris buffer solution and then vortexed, centrifuged, and incubated at about 0 °C for at least 6 h. Several DSC scans were performed at a nominal rate of 10 °C/h on each sample. The first scan for each sample was discarded. For each scan presented, therefore, the sample had previously been slowly cycled throught the transition at least once. Typically, the scans presented are the third or fourth carried out on a given sample. Little variation in the DSC trace from scan to scan is observed after the first scan. This suggests that, for these samples, the first slow cycle through the transition is adequate to ensure equilibrium hydration for subsequent scans. DSC scans were performed on a Microcal MC1 high-sensitivity differential scanning calorimeter and analyzed as described elsewhere (Morrow et al., 1985).

Results and Discussion

Figure 2 shows DSC scans and transition enthalpies for the series of gramicidin–DPPC-d_{62} mixtures up to a gramicidin concentration of x = 0.025. These scans show a distinct broadening of the transition to lower temperature reminiscent of the observation for lipid–synthetic peptide mixtures in which two-phase coexistence is seen. The transition region does not straddle the temperature of the pure lipid transition to the extent seen with the mixtures, discussed below, containing DMPC. The transition enthalpy decreases with increasing gramicidin concentration in the manner often seen for lipid–protein mixtures.

^{2}H NMR spectra covering the temperature range from 16 to 50 °C were obtained for each gramicidin–DPPC-d_{62} sample.

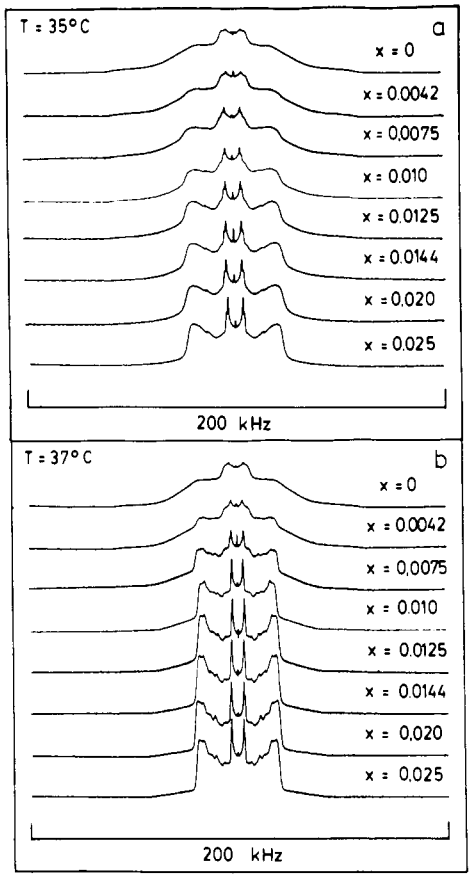

FIGURE 3: Concentration dependence of ^2H NMR spectra for gramicidin–DPPC-d_{62} multilamellar vesicles at (a) 35 °C and (b) 37 °C.

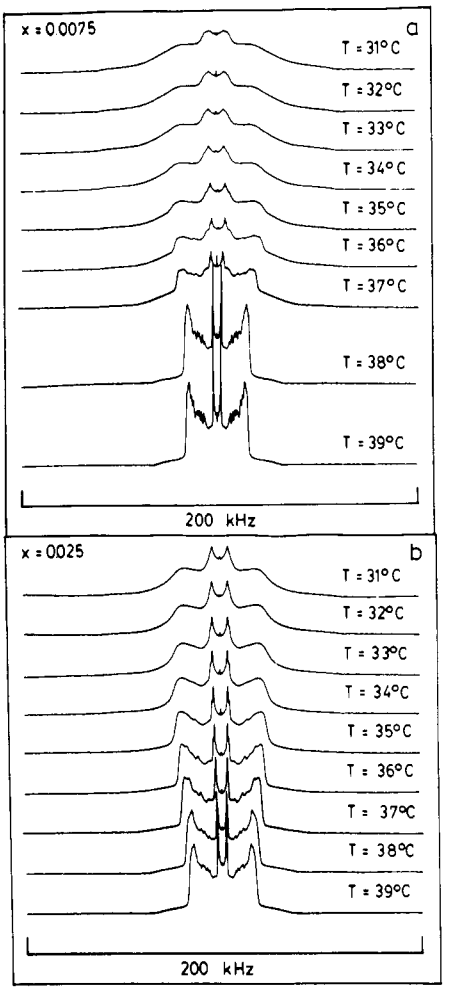

FIGURE 4: Temperature dependence of ^2H NMR spectra for gramicidin–DPPC-d_{62} multilamellar vesicles at gramicidin mole fractions of (a) $x = 0.0075$ and (b) $x = 0.025$.

Above 37 °C, the component powder patterns are characteristic of axially symmetric motion, and the resulting superposition is the distinctive liquid-crystal spectrum. At low temperature, the spectra are characteristic of the slower, nonaxially symmetric motion in the gel phase.

Both types of experiment show the downward shift in transition temperature of perdeuteriated lipids relative to the transition temperature of the normal lipid. For DPPC-d_{62}, the shift is approximately 4 °C while for DMPC-d_{54} the shift is approximately 3 °C. This isotope effect is well-known for perdeuteriated lipids (Davis, 1979). There is good reason to believe that the qualitative features of lipid phase behavior are not significantly altered by perdeuteriation. For example, the pretransition and main transition bear the same relation in the perdeuteriated lipid as in the normal lipid. The effect of perdeuteriation on the phase behavior of a lipid can be examined by comparing the spectra of selectively labeled lipid, for which the isotope effect should be negligible, to the corresponding features in the spectra of perdeuteriated lipid. Such comparison (Davis, 1979) indicates no qualitative change in the thermotropic behavior or hydrocarbon flexibility gradient of the lipid on perdeuteriation.

Two possibilities exist for spectra just below the pure lipid transition temperature. For combinations of temperature and composition within a region of two-phase coexistence, spectra will be a superposition of gel and liquid-crystal contributions if lipid exchange between phase domains is slow. The component spectra correspond to compositions, for that temperature, at the boundaries of the two-phase region and are referred to as end-point spectra.

The other possibility for spectra in the transition region is that they might not be resolvable into distinct gel and liquid-crystal components. This might arise, for example, if the time for lipid exchange between domains of coexisting phase is short compared to the inverse of the spectral splitting. The inability to resolve gel and liquid-crystal components might also indicate the occurrence of a region of continuous phase change rather than a transition via two-phase coexistence.

Figure 3 shows the concentration dependence of deuterium NMR spectra for the same gramicidin–DPPC-d_{62} mixtures at 35 and 37 °C. The liquid-crystal–gel transition in the pure perdeuteriated lipid occurs between 37 and 38 °C. For both temperatures shown in Figure 3, the spectra for $x = 0.0042$ and for $x = 0.0075$ show distinct contributions from coexisting gel and liquid-crystal phases. Figure 4 shows the temperature dependence of the deuterium NMR spectrum for the mixtures with $x = 0.0075$ and $x = 0.025$. It is apparent that, for the lower concentration shown, two-phase coexistence exists from 35 to 37 °C. Above this range, the sample is liquid-crystal. There may be a small liquid-crystal contribution to the $x = 0.0075$, $T = 34$ °C spectrum, but the spectra below this temperature for the lower concentration are characteristic of the gel phase. The series for $x = 0.025$, however, does not contain any spectra showing distinct contributions from coexisting gel and liquid-crystal phases. Rather, this series displays a continuously increasing degree of order.

The temperature dependence of M_1 for the gramicidin–DPPC-d_{62} series is shown in Figure 5. Gramicidin is seen to have a strong disordering effect just below the transition temperature and a weaker ordering effect just above the pure lipid transition temperature. Knowledge of M_1, and thus the

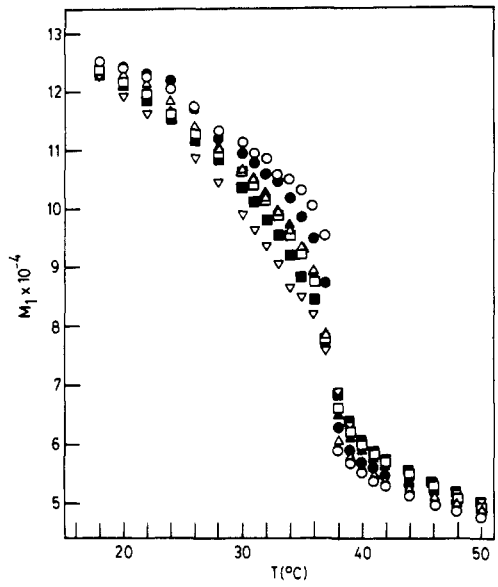

FIGURE 5: Temperature dependence of the first moment of ^2H NMR spectra of gramicidin–DPPC-d_{62} mixtures at different gramicidin mole fractions. Spectra were obtained with a quadrupole echo delay of 35 μs. (○) $x = 0.0042$; (●) $x = 0.0075$; (△) $x = 0.010$; (▲) $x = 0.013$; (□) $x = 0.014$; (■) $x = 0.020$; (▽) $x = 0.025$.

average orientational order parameter (Davis, 1979), permits the approximate calculation of the thickness of the hydrophobic region of the bilayer as a function of gramicidin content (Schindler & Seelig, 1975). At 40 °C, M_1 goes from 5.5 × 10^4 s^{-1} for pure DPPC-d_{62} to 6.0 × 10^4 s^{-1} for 2.5 mol % gramicidin. This corresponds to a change in hydrophobic thickness from 25.6 to 26.2 Å.

Both the calorimetric and spectroscopic evidence presented suggest that the gramicidin–DPPC-d_{62} mixtures display a region of two-phase coexistence from the pure lipid transition temperature down to and including approximately 35 °C. This region may include $x = 0.020$ but does not appear to extend up to $x = 0.025$. Spectral difference analysis (Huschilt et al., 1985) was applied to pairs of spectra in this region. By use of this technique, end-point spectra and corresponding boundary compositions may be obtained by taking differences of spectra from within the two-phase region at a given temperature. Within a two-phase region of a binary phase diagram, the compositions of the coexisting phases are given by the end points of an isothermal tie line drawn between the two boundaries. The fraction of sample in each phase is given by the lever rule. If the end points at a given temperature correspond to gel at solute mole fraction x_{gel} and liquid-crystal at x_{lc}, then the fraction of the sample in the gel phase is

$$F_g = (x_{lc} - x)/(x_{lc} - x_{gel})$$

where x is the overall sample composition. ^2H NMR spectra within a two-phase region will thus be superpositions of gel and liquid-crystal components with the proportions determined by the lever rule. Given two spectra at the same temperature but different overall composition, an appropriate factor times one spectrum can be subtracted from another to obtain the gel or liquid-crystal end-point spectra. From the lever rule and the factor used in the subtraction, it is possible to infer the end-point compositions for that temperature. In the present case, however, the small concentration range over which distinct two-component spectra are observable prevents precise determination of phase boundaries using this method. An example of the spectral subtractions at 36 °C is shown in Figure 6. Spectra b and c, respectively, correspond to $x = 0.010$ and $x = 0.0042$. Spectrum d is obtained by subtracting

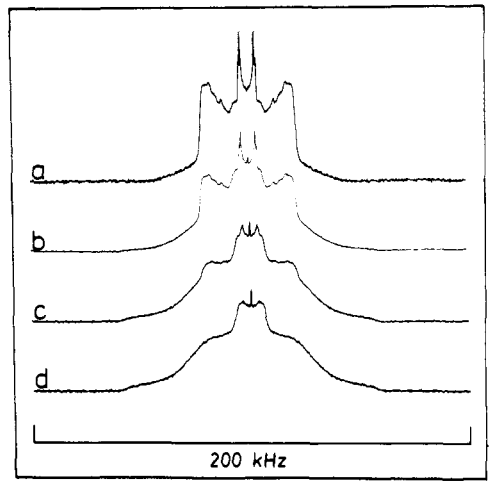

FIGURE 6: Extraction of end-point spectra from two gramicidin–DPPC-d_{62} spectra at the same temperature but different concentrations within the two-phase region at $T = 36$ °C. (a) Fluid-phase end-point spectrum corresponding to $x = 0.017$ obtained by subtracting 0.529 times spectrum c from spectrum b. (b) Two-component spectrum at $x = 0.01$. (c) Two-component spectrum at $x = 0.0042$. (d) Gel-phase end-point spectrum corresponding to $x = 0.0015$ obtained by subtracting 0.278 times spectrum b from spectrum c.

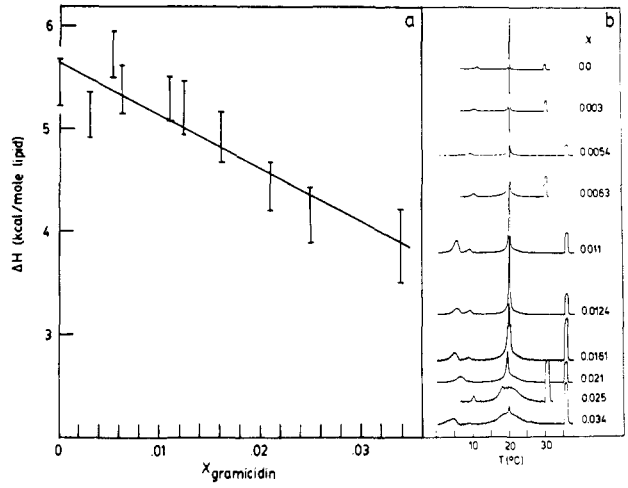

FIGURE 7: DSC results for a series of gramicidin–DMPC-d_{54} multilamellar vesicle samples. (a) Transition enthalpy per mole of lipid versus gramicidin mole fraction. (b) DSC traces for this series. Each trace ends with a calibration pulse.

0.278 times spectrum b from spectrum c. The analysis presented in Huschilt et al. (1985) indicates that this result corresponds to a gel boundary between $x = 0.001$ and $x = 0.002$. Spectrum a is obtained by subtracting 0.529 times spectrum c from spectrum b. The analysis yields a liquid-crystal boundary between $x = 0.016$ and $x = 0.018$. Other subtractions place this boundary as high as $x = 0.022$ or as low as $x = 0.014$. While the precision in this result is low, presumably for the reason suggested above, the ability to perform the subtraction at all is evidence for two-phase coexistence in this region of the phase diagram.

Thus, DPPC-d_{62}–gramicidin mixtures appear to display a phase diagram consisting of a narrow region of two-phase coexistence surrounded by a region of continuous phase change. The temperature range over which two-phase coexistence is supported is about 3 °C while the limit in concentration, both from spectral subtraction at 36 °C and from inspection, seems to be in the neighborhood of $x = 0.02$.

A corresponding set of experiments carried out on mixtures of gramicidin with DMPC-d_{54} shows subtle differences from the DPPC–gramicidin mixtures. Figure 7 shows DSC scans

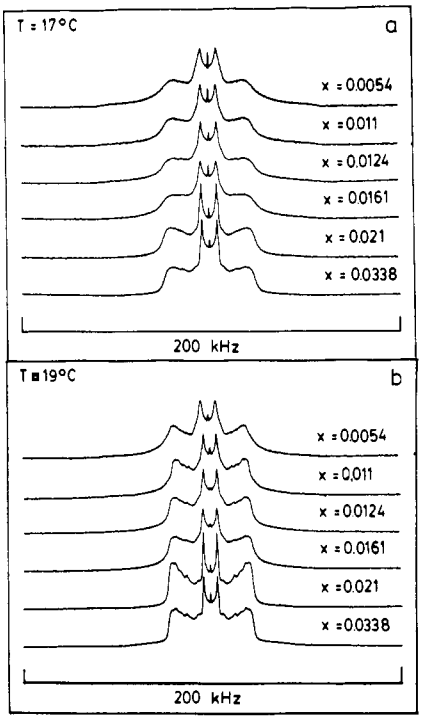

FIGURE 8: Concentration dependence of the ^2H NMR spectrum for gramicidin–DMPC-d_{54} multilamellar vesicles at (a) 17 °C and (b) 19 °C.

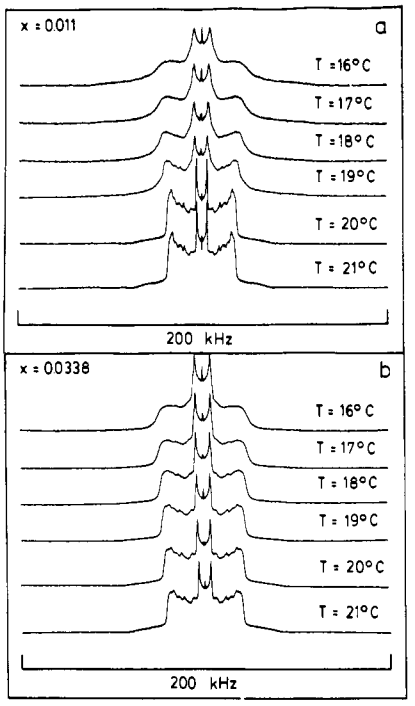

FIGURE 9: Temperature dependence of the ^2H NMR spectrum for gramicidin–DMPC-d_{54} multilamellar vesicles at gramicidin mole fractions of (a) $x = 0.011$ and (b) $x = 0.034$.

and transition enthalpies for a series of DMPC-d_{54}–gramicidin mixtures up to $x = 0.034$. These scans are roughly symmetric up to 1.2 mol % gramicidin and appear to straddle the pure lipid transition temperature for all concentrations. This contrasts with the situation for synthetic peptide–DPPC mixtures in which broadening of the transition occurs primarily on the low-temperature side of the pure lipid transition, resulting in asymmetric traces which are taken to be characteristic of two-phase coexistence (Morrow et al., 1985). The scan for $x = 0.016$ shows a small shoulder on the high-temperature side of the peak. This behavior was confirmed by making a second sample at $x = 0.015$. Simulation of DSC scans (Mabrey & Sturtevant, 1976; Morrow et al., 1985) suggests that vertical edges in the calorimetry scan (which will appear somewhat rounded in actual experiments) may be associated with boundaries of two-phase coexistence regions in the phase diagram. It is thus possible that near $x = 0.015$, the gramicidin–DMPC phase diagram displays a two-phase region with a width of about 1 °C. At $x = 0.021$, this two-phase region would appear to have narrowed again, so the separation of the edges is not resolved. The two highest concentrations show no sign of a sharp phase boundary and are more indicative of a continuous phase change. Again, the transition enthalpy decreases linearly with increasing gramicidin concentration.

It is interesting to note that the presence of gramicidin in DMPC seems to promote the appearance of a subtransition near 5 °C. The DMPC subtransition had previously been observed only following extended cold incubation (Finegold & Singer, 1986; Singer & Finegold, 1985).

Figures 8 and 9 display representative ^2H NMR spectra in the neighborhood of the DMPC-d_{54} phase change. Figure 8 shows the concentration dependence of ^2H NMR spectra for a series of gramicidin–DMPC-d_{54} mixtures at two temperatures near the pure lipid transition temperature. At 19 °C (Figure 8b), the sample with gramicidin mole fraction $x = 0.011$ shows distinct evidence of two-phase coexistence. For a lower gramicidin concentration, $x = 0.0054$, the spectrum at 19 °C primarily indicates gel phase although there may be a small amount of coexisting liquid-crystal. As the concentration of gramicidin is increased beyond $x = 0.011$, the spectra become increasingly indicative of the liquid-crystalline phase but are not easily resolvable into gel and liquid-crystalline components. At 18 °C, the trend toward liquid-crystal-like spectra appears, even more, to proceed by a continuous change in the spectral shape rather than through a series of spectra displaying coexistence of gel and liquid-crystal. At 17 °C (Figure 8a), increasing gramicidin concentration results in a continuous narrowing of the spectra, indicating a decrease in chain order with increasing gramicidin content, but no liquid-crystalline spectrum is obtained in the range of concentrations studied.

Figure 9 shows the temperature dependence of ^2H NMR spectra for these mixtures at two concentrations. For $x = 0.011$, the transition from gellike to liquid-crystal-like spectra occurs over a narrow range in temperature. Again, the most distinct evidence for a region of two-phase coexistence is the spectrum at $T = 19$ °C for the concentration $x = 0.011$ (Figure 9a). The series at higher gramicidin concentration, $x = 0.034$ (Figure 9b), is qualitatively different. As the temperature is lowered, the spectra broaden and lose the sharp features associated with 90° edges in the liquid-crystalline spectra. The change, however, is continuous and shows no evidence of two-phase coexistence. The broad wings characteristic of the gel phase are not prominent even in the spectrum at 16 °C.

Spectral difference analysis (Huschilt et al., 1985) was also performed on gramicidin–DMPC-d_{54} spectra at 19 and 18 °C. At 19 °C, the subtractions suggest a liquid-crystal boundary near $x = 0.02$, but the resulting end-point spectra are not consistent with the liquid-crystal spectrum measured directly for $x = 0.021$. At 18 °C, no consistent liquid-crystal end-point spectrum is obtained from spectral subtraction. These negative results confirm that the gramicidin–DMPC-d_{54} spectra at 18 and 19 °C are not cleanly resolvable into distinct gel and liquid-crystal contributions.

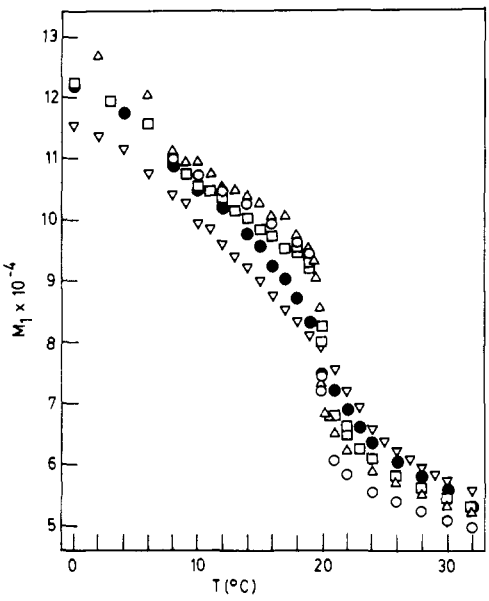

FIGURE 10: Temperature dependence of the first moment of ^2H NMR spectra for gramicidin–DMPC-d_{54} mixtures at different gramicidin mole fractions. Spectra were obtained by using a quadrupole echo delay of 35 μs. (○) x = 0.0; (△) x = 0.003; (□) x = 0.006; (●) x = 0.015; (▽) x = 0.025.

Figure 10 shows the temperature dependence of the first spectral moment, M_1, for a series of gramicidin concentrations. The spectra used for this figure were obtained by using a quadrupolar echo delay time (τ) of 35 μs. The transition from liquid-crystal to gel at low gramicidin concentration results in a sharp increase in M_1 corresponding to the increase in chain order at the transition. From the dependence of M_1 on gramicidin content both above and below 20 °C, it is apparent that the ordering effect of gramicidin on DMPC above the pure lipid transition temperature is as prominent as its disordering effect below. This differs from the case for DPPC (Figure 5), where the effect of gramicidin on M_1 is stronger below the lipid transition temperature than above. The gramicidin–DMPC results are also in contrast with those reported for some protein–lipid (Bienvenue et al., 1982; Paddy et al., 1981) and peptide–lipid (Huschilt et al., 1985) mixtures where the effect of protein on M_1 above the transition is small. We can again estimate the effect of gramicidin on the hydrophobic thickness of DMPC in the liquid-crystalline phase. From Figure 10, M_1 at 24 °C goes from 5.6 × 10^4 s^{-1} for pure DMPC-d_{54} to 6.6 × 10^4 s^{-1} for a gramicidin mole fraction of 0.034. According to the approximate calculation of Schindler and Seelig (1975), this change in M_1 is found to correspond to a change in hydrophobic thickness from 22.3 to 23.3 Å.

In Figure 10, the highest concentration, x = 0.025, shows a continuous increase in order with no sharp boundary between gellike and liquid-crystal-like behavior. The phase change apparently occurs over a temperature range centered on the pure lipid transition temperature. It must be noted, however, that for equilibrium two-component phase diagrams the boundaries of a region of two-phase coexistence must approach the pure component axis with slopes having the same sign. A consequence of this rule is that, in the limit of small solute concentration, two-phase regions which straddle the transition temperature of the pure solvent, in our case lipid, are disallowed on thermodynamic grounds. Accordingly, some care must be taken in interpreting the range in temperature over which M_1 is observed to change and over which the excess heat capacity is observed, by DSC, to depart from its base-line value.

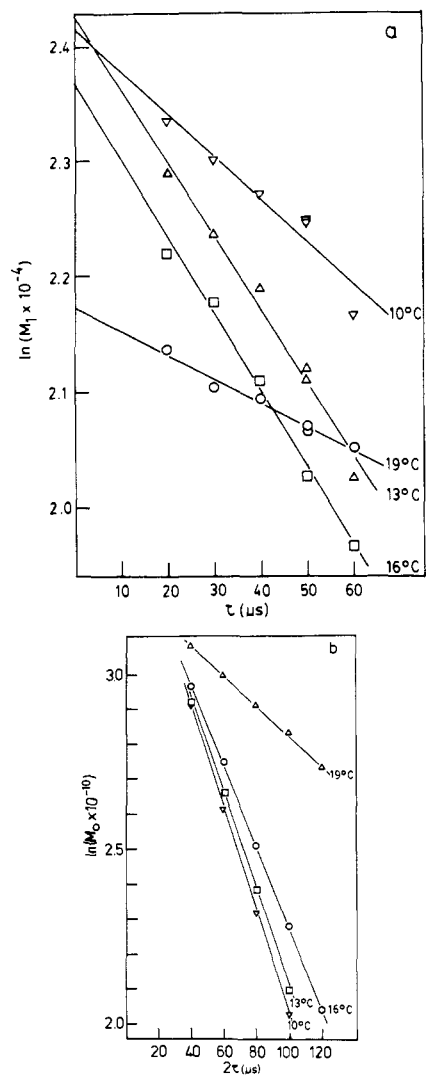

FIGURE 11: (a) Quadrupole echo delay time dependence of the first moment of ^2H NMR spectra for gramicidin–DMPC-d_{54} at 3.4 mol % gramicidin for four temperatures. The slopes for 10, 13, 16, and 19 °C, respectively, are −3700, −6400, −6799, and −2100 s^{-1}. (b) Semilog plot of integrated spectral intensity versus quadrupole echo delay for four temperatures. T_{2e} for 19 °C is 230 μs and for 16 °C, 86 μs.

^2H NMR spectra were also obtained for a series of gramicidin–DMPC-d_{54} mixtures using a delay time of τ = 50 μs. Above 19 °C, the dependence of the moments on temperature and gramicidin content is the same as for the shorter echo delay time. At 19 °C, there is a sharp break in the plot of M_1 versus temperature for x = 0.021 and x = 0.034. This reflects a strong τ dependence of the line shape for larger gramicidin concentrations in the gel phase. Figure 11a displays the τ dependence of the first spectral moment in this region as a function of temperature for 3.4 mol % gramicidin in DMPC-d_{54}. The sensitivity of M_1 to τ passes through a maximum between 13 and 16 °C. Figure 11b shows that this behavior coincides with a sharp decrease, but not a minimum, in the quadrupole echo decay time, T_{2e}. At 19 °C, T_{2e} is 230 μs. By 16 °C, T_{2e} has decreased to 86 μs. The τ dependence of M_1 reflects the extent to which echo components corresponding to the wings of the spectrum decay more quickly than those associated with the center of the spectrum. With perdeuteriated lipids, this dependence may reflect a variation of T_{2e} with molecular orientation or a variation with position along the chain. Further experiments using mixtures of gramicidin with specifically deuteriated DMPC will be needed

to distinguish these possibilities.

Both the calorimetric and spectroscopic results described on the gramicidin–DMPC-d_{54} system suggest that the phase diagram contains a two-phase region covering about 1 °C in temperature and extending from $x = 0$ to between $x = 0.020$ and $x = 0.025$. Beyond these limits is a region of continuous phase change. A two-phase boundary of this shape implies the existence of a critical mixing point (consolute point) (Rowlinson & Swinton, 1982; Haase & Schonert, 1969; van Konyenburg & Scott, 1980), at the lowest temperature limit of two-phase coexistence as illustrated in Figure 1. The phase diagrams for DMPC–gramicidin and for DPPC–gramicidin mixtures seem to differ primarily through the width, in temperature, of the coexistence region.

Conclusions

Some difficulties exist in trying to infer continuous phase behavior from the absence of distinct two-component spectra. The inability to resolve two components in the spectrum might also result from the presence of fast lipid exchange between domains of gel and liquid-crystal. For both systems, increasing x at a temperature less than 1 °C below the pure lipid transition results in the crossing of a region in which two distinct spectral contributions may be resolved. The same process carried out 2 °C lower yields spectra with no cleanly resolvable gel and liquid-crystal contributions. It is difficult to see how the rate of exchange between domains could be significantly increased due to cooling. However, it is possible that the size of the domains might decrease to the point where exchange could obscure distinct contributions to the spectrum. Similarly, changing T at low polypeptide concentration yields a region of resolvable two-component spectra. Above $x = 0.02$, the same process fails to yield distinct two-component spectra. Again, gel–liquid-crystal exchange might account for this observation. As discussed below, however, the calorimetry scans appear to be consistent with a picture of two-phase coexistence giving way to a region of continuous phase change. The use of specifically labeled lipid might aid in distinguishing these possibilities since two-component contributions to a spectrum would be more readily apparent in the simpler spectra. Such spectra would also lend themselves more readily to simulation studies of the spectra characteristic of gel–liquid-crystal exchange. Further, they may indicate whether this process could explain the spectra in the region of apparently continuous phase change. Simulation of specific label spectra might also be helpful in understanding the unusual shape of the low-temperature, high gramicidin content spectra of DMPC-based mixtures such as the $T = 16$ °C spectrum of Figure 9b. The use of specifically labeled lipid in such a study would also provide a control for any possible effect of perdeuteriation on lipid–peptide interaction.

A phase diagram of the type shown in Figure 1 would reconcile the apparent discrepancy between some DSC results and the rules for equilibrium two-component phase diagrams. DSC results both in this study and in previous work on higher peptide concentrations of DPPC-d_{62}–synthetic peptide mixtures show excess heat capacity beyond the spectroscopically observed region of two-phase coexistence and, in some cases, above the pure lipid transition temperature. As discussed above, the rules for equilibrium two-component phase diagrams effectively prohibit straddling of the pure lipid transition temperature by a region of two-phase coexistence and suggest that the observation of excess heat capacity beyond the pure lipid transition temperature arises from a region of continuous phase change. The presence of a critical mixing point would account for such a region at high polypeptide concentration. At concentrations beyond the limit of two-phase coexistence, the continuous phase change should yield a broad maximum in excess heat capacity. As concentration is lowered, the two-phase region will be encountered, but vestiges of the continuous phase change must persist above and below the two-phase region. The resulting DSC scan will show sharp features, associated with crossing of phase boundaries, sandwiched between broad regions of excess heat capacity. As concentration is further lowered, the transition occurs further from the critical concentration, and the broad features should diminish, leaving sharp two-phase features. This progression is seen in the present study and in the synthetic peptide work. The phase diagrams for the latter systems (Huschilt et al., 1985) seem, in fact, to be tending toward a critical point near $T = 27$ °C and $x = 0.05$. Studies on the synthetic peptide system at higher concentration would be a useful test for the presence of a critical point in this system.

The role of lipid chain length in determining the extent of two-phase coexistence is clouded by the likelihood of the dimer–monomer equilibrium being different in the two lipids. It is possible that this equilibrium is coupled to the phase transition through the change in bilayer thickness at the transition. If the effect of the polypeptide is primarily a lateral perturbation of independent bilayer halves, one might not expect the phase behavior to be sensitive to monomer–dimer equilibrium. These results would then suggest that the longer lipid, DPPC, is better able to support two-phase coexistence in the presence of the polypeptide. If, on the other hand, bilayer–peptide hydrophobic mismatch stresses the bilayer, as suggested by the "mattress model" of Mouritsen and Bloom (1984), then the difference in the extent of two-phase coexistence observed with the two lipids might reflect a shift in monomer–dimer equilibrium. Wallace et al. (1981) suggest from circular dichroism evidence that the conformations of gramicidin in DPPC and in DSPC are similar. Presumably, gramicidin–lipid mixtures based on DSPC and DPPC would experience similar monomer–dimer equilibrium effects allowing them to be separated from bilayer thickness effects. If the synthetic peptide system also proves to display this type of phase diagram, studies with a variety of lipids might also provide a means to examine the sensitivity of critical concentration to bilayer thickness.

In summary, DSC and ^{2}H NMR experiments have been performed on gramicidin–DPPC-d_{62} and gramicidin–DMPC-d_{54} mixtures. The results suggest that both mixtures display a region of two-phase coexistence just below the pure lipid transition temperature. Beyond about 2 mol %, two-phase coexistence gives way to continuous phase change, implying the presence of a critical mixing point. The existence of such a feature in the phase diagram is consistent with the observation of broad, featureless peaks in DSC scans at the higher gramicidin concentrations. The first moment, M_1, of ^{2}H NMR spectra of DMPC-d_{54} in the liquid-crystalline phase is found to be more sensitive to gramicidin concentration than has been seen for other protein–lipid systems. Finally, the sharp minimum in the M_1 "decay time" just below the pure lipid transition calls for further study. The use of specifically labeled lipids in a study of line-shape dependence on quadrupole echo delay time would separate the orientation dependence of T_{2e} from a sensitivity to position along the chain. This would be a useful step in characterizing the change in lipid dynamics observed at the transition for gramicidin-rich bilayers.

Acknowledgments

We thank Myer Bloom, J. P. Whitehead, and J. V. Sengers for useful discussions.

Registry No. DPPC, 63-89-8; DMPC, 18194-24-6; gramicidin, 1405-97-6.

REFERENCES

Abney, J. R., & Owicki, J. C. (1985) in *Progress in Protein–Lipid Interactions* (Watts, A., & De Pont, J. J. H. H. M., Eds.) pp 1–60, Elsevier Science, Amsterdam.

Arseniev, A. S., Barsukov, I. L., Bystrov, V. F., Lomize, A. L., & Ovchinnikov, Yu. A. (1985) *FEBS Lett. 186*, 168–174.

Bienvenue, A., Bloom, M., Davis, J. H., & Devaux, P. F. (1982) *J. Biol. Chem. 257*, 3032–3038.

Bloom, M., & Smith, I. C. P. (1985) in *Progress in Protein–Lipid Interactions* (Watts, A., & De Pont, J. J. H. H. M., Eds.) pp 61–88, Elsevier Science, Amsterdam.

Chapman, D., Cornell, B. A., Eliasz, A. W., & Perry, A. (1977) *J. Mol. Biol. 113*, 517–538.

Cheng, W. H. (1980) *Biochim. Biophys. Acta 600*, 358–366.

Cornell, B. A., Davenport, J. B., & Separovic, F. (1982) *Biochim. Biophys. Acta 689*, 337–345.

Davis, J. H. (1979) *Biophys. J. 27*, 339–358.

Davis, J. H. (1986) *Chem. Phys. Lipids 40*, 223–258.

Devaux, P. F., & Seigneuret, M. (1985) *Biochim. Biophys. Acta 822*, 63–125.

Elliot, J. R., Needham, D., Dilger, J. P., & Haydon, D. A. (1983) *Biochim. Biophys. Acta 735*, 95–103.

Finegold, L., & Singer, M. A. (1986) *Biochim. Biophys. Acta 855*, 417–420.

Friere, E., Markello, T., Rigell, C., & Holloway, P. W. (1983) *Biochemistry 22*, 1675–1680.

Griffith, O. H., McMillen, D. A., Keana, J. F. W., & Jost, P. C. (1986) *Biochemistry 25*, 574–584.

Gupta, C. M., Radhakrishnan, R., & Khorana, H. G. (1977) *Proc. Natl. Acad. Sci. U.S.A. 74*, 4315–4319.

Haase, R., & Schonert, H. (1969) *Solid–Liquid Equilibrium*, Pergamon, Oxford.

Heyn, M. P., Blume, A., Rehorek, M., & Dencher, N. A. (1981) *Biochemistry 20*, 7109–7114.

Huschilt, J. C., Hodges, R. S., & Davis, J. H. (1985) *Biochemistry 24*, 1377–1386.

Lee, A. G. (1977) *Biochim. Biophys. Acta 472*, 285–344.

Lee, D. C., Durrani, A. A., & Chapman, D. (1984) *Biochim. Biophys. Acta 769*, 49–56.

Mabrey, S., & Sturtevant, J. M. (1976) *Proc. Natl. Acad. Sci. U.S.A. 73*, 3862–3866.

Meirovitch, E., Nayeem, A., & Freed, J. H. (1984) *J. Phys. Chem. 88*, 3454–3465.

Mendelsohn, R., Brauner, J. W., Faines, L., Mantsch, H. H., & Dluhy, R. A. (1984) *Biochim. Biophys. Acta 774*, 237–246.

Morrow, M. R., Huschilt, J. C., & Davis, J. H. (1985) *Biochemistry 24*, 5396–5406.

Mouritsen, O. G., & Bloom, M. (1984) *Biophys. J. 46*, 141–153.

Paddy, M. R., Dahlquist, F. W., Davis, J. H., & Bloom, M. (1981) *Biochemistry 20*, 3152–3162.

Pink, D. A., & Chapman, D. (1979) *Proc. Natl. Acad. Sci. U.S.A. 76*, 1542–1546.

Ramsay, G., Prabhu, R., & Friere, E. (1986) *Biochemistry 25*, 2265–2270.

Rehorek, M., Dencher, N. A., & Heyn, M. P. (1985) *Biochemistry 24*, 5980–5988.

Rice, D., & Oldfield, E. (1979) *Biochemistry 18*, 3272–3279.

Ring, A. (1986) *Biochim. Biophys. Acta 856*, 646–653.

Rowlinson, J. S., & Swinton, F. L. (1982) *Liquids and Liquid Mixtures*, Butterworth Scientific, London.

Schindler, H., & Seelig, J. (1975) *Biochemistry 14*, 2283–2287.

Scott, H. L., & Cheng, W. H. (1979) *Biophys. J. 28*, 117–132.

Semin, B. K., Saraste, M., & Wikstrom, M. (1984) *Biochim. Biophys. Acta 769*, 15–22.

Singer, M. A., & Finegold, L. (1985) *Biochim. Biophys. Acta 816*, 303–312.

Streett, W. B. (1974) *Can. J. Chem. Eng. 52*, 92–97.

Tanaka, H., & Freed, J. H. (1985) *J. Phys. Chem. 89*, 350–360.

Tenchov, B. G. (1985) *Prog. Surf. Sci. 20*, 273–340.

Urry, D. W., Trapane, T. L., & Prasad, K. U. (1983) *Science (Washington, D.C.) 221*, 1064–1067.

van Konyenburg, P. H., & Scott, R. L. (1980) *Philos. Trans. R. Soc. London, A 298*, 495–540.

Wallace, B. A. (1986) *Biophys. J. 49*, 295–306.

Wallace, B. A., Veatch, W. R., & Blout, E. R. (1981) *Biochemistry 20*, 5754–5760.

Weinstein, S., Durkin, J. T., Veatch, W. R., & Blout, E. R. (1985) *Biochemistry 24*, 4374–4382.